

Supplement S3

February 14, 2022

1 Catchment data

The conceptual hydrological models FLEX, TUWmodel and GR4J were calibrated and run with increased precipitation for the CAMELS-data and several Australian catchments.

1.1 Australian catchments

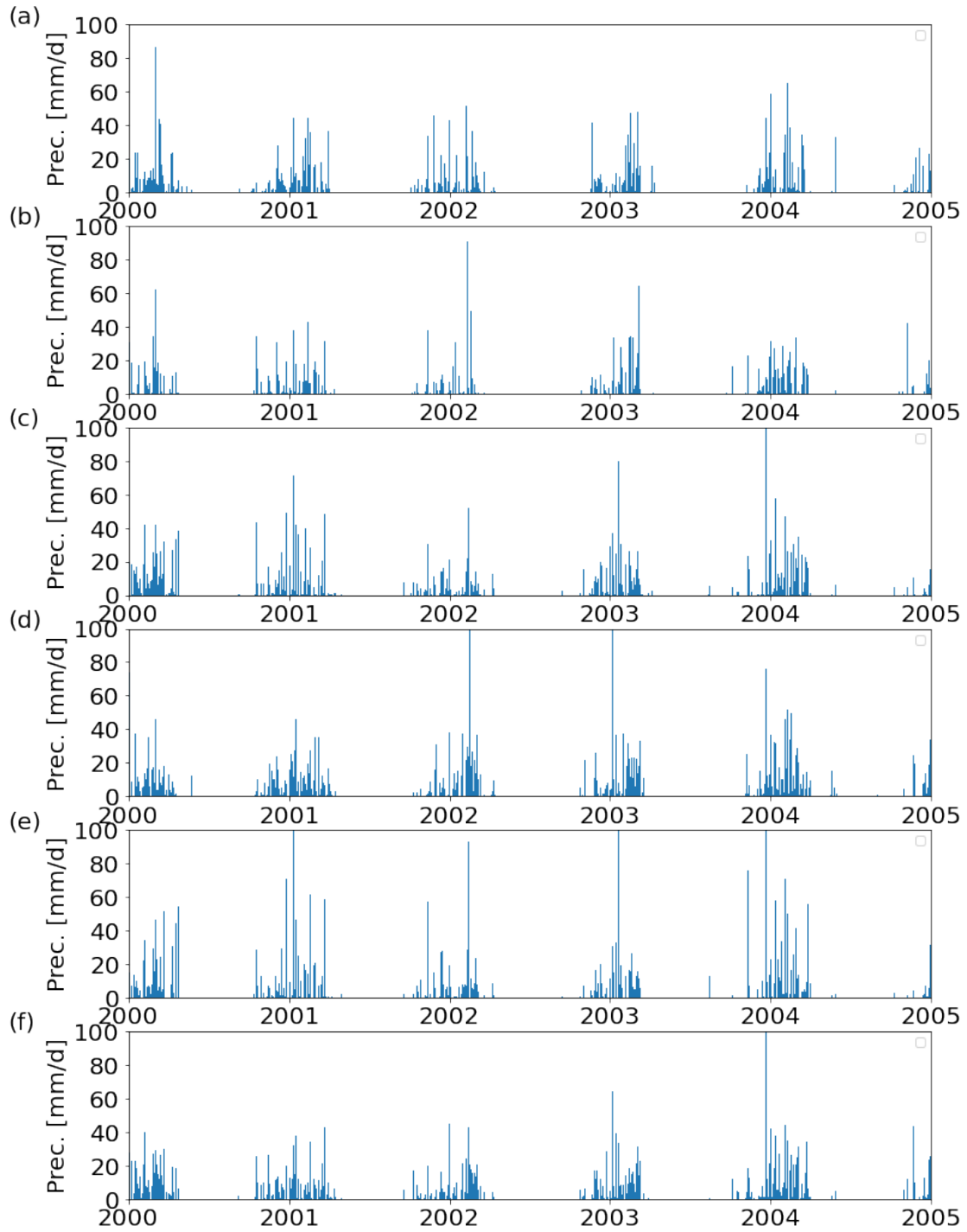


Fig. S3.1. Precipitation time series for a) Adelaide River, b) Dry River, c) Fergusson River, d) Magela Creek, e) Seventeen Mile Creek and f) South Alligator River.

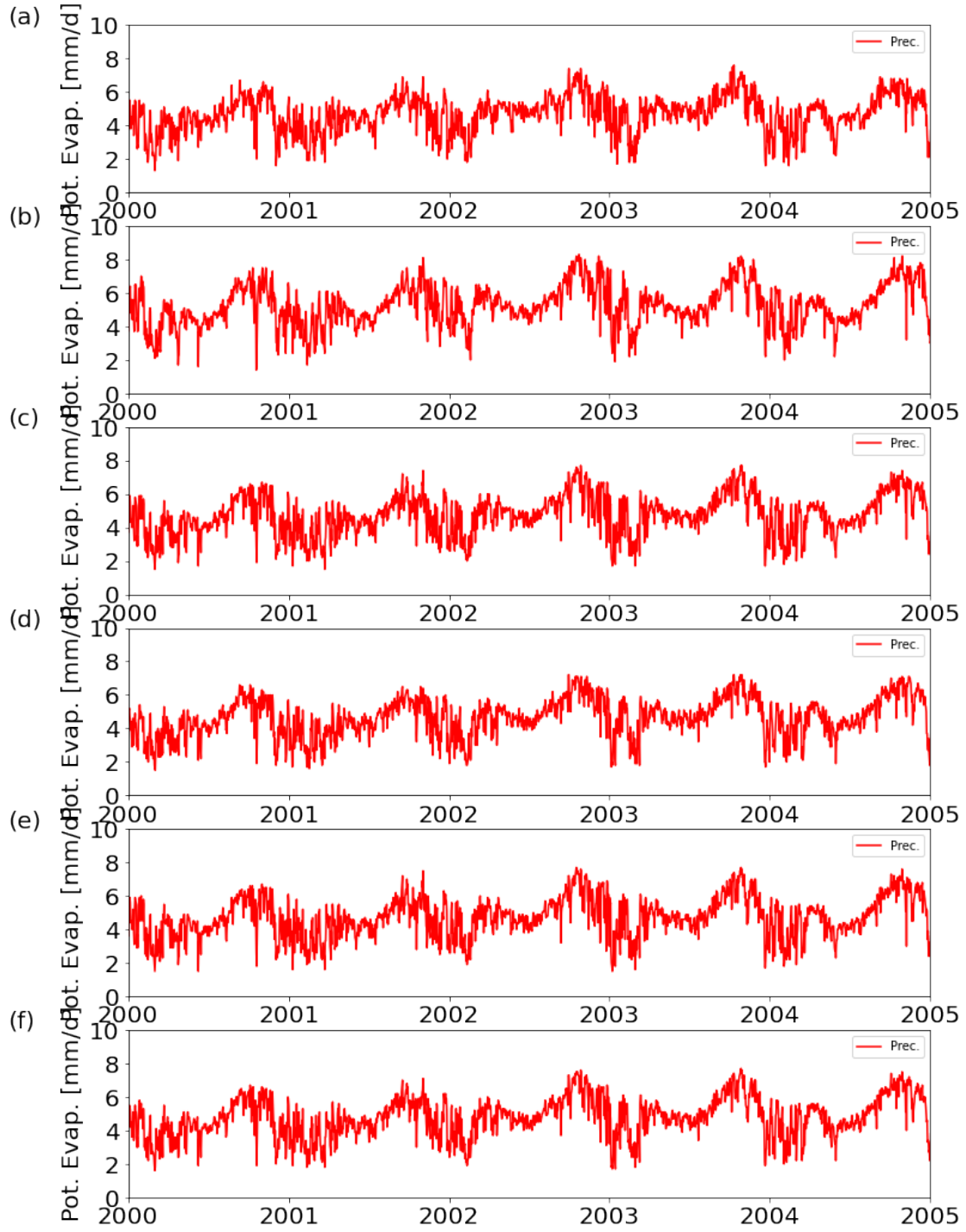


Fig. S3.2. Potential evaporation time series for a) Adelaide River, b) Dry River, c) Fergusson River, d) Magela Creek, e) Seventeen Mile Creek and f) South Alligator River.

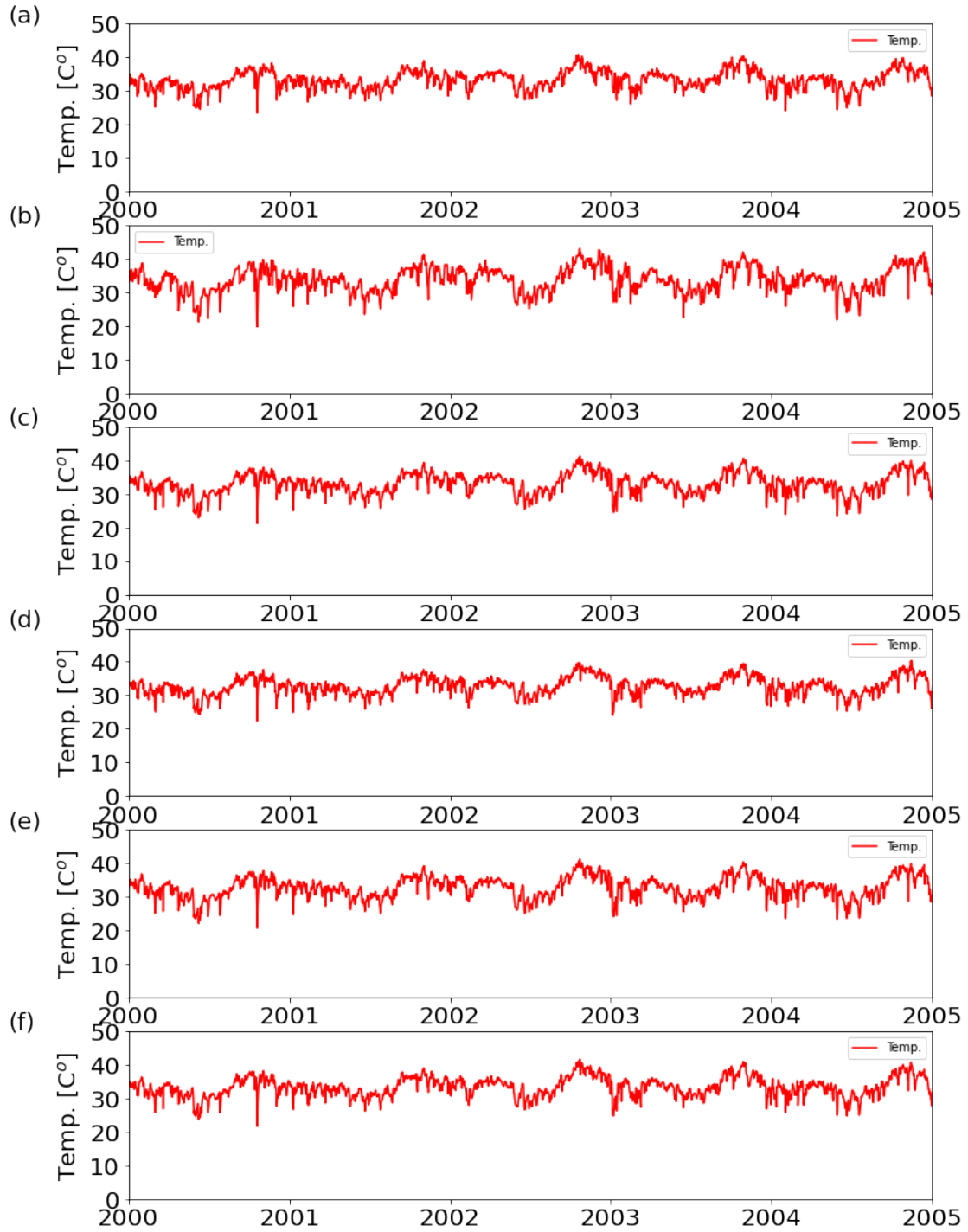


Fig. S3.3. Temperature time series for a) Adelaide River, b) Dry River, c) Fergusson River, d) Magela Creek, e) Seventeen Mile Creek and f) South Alligator River.

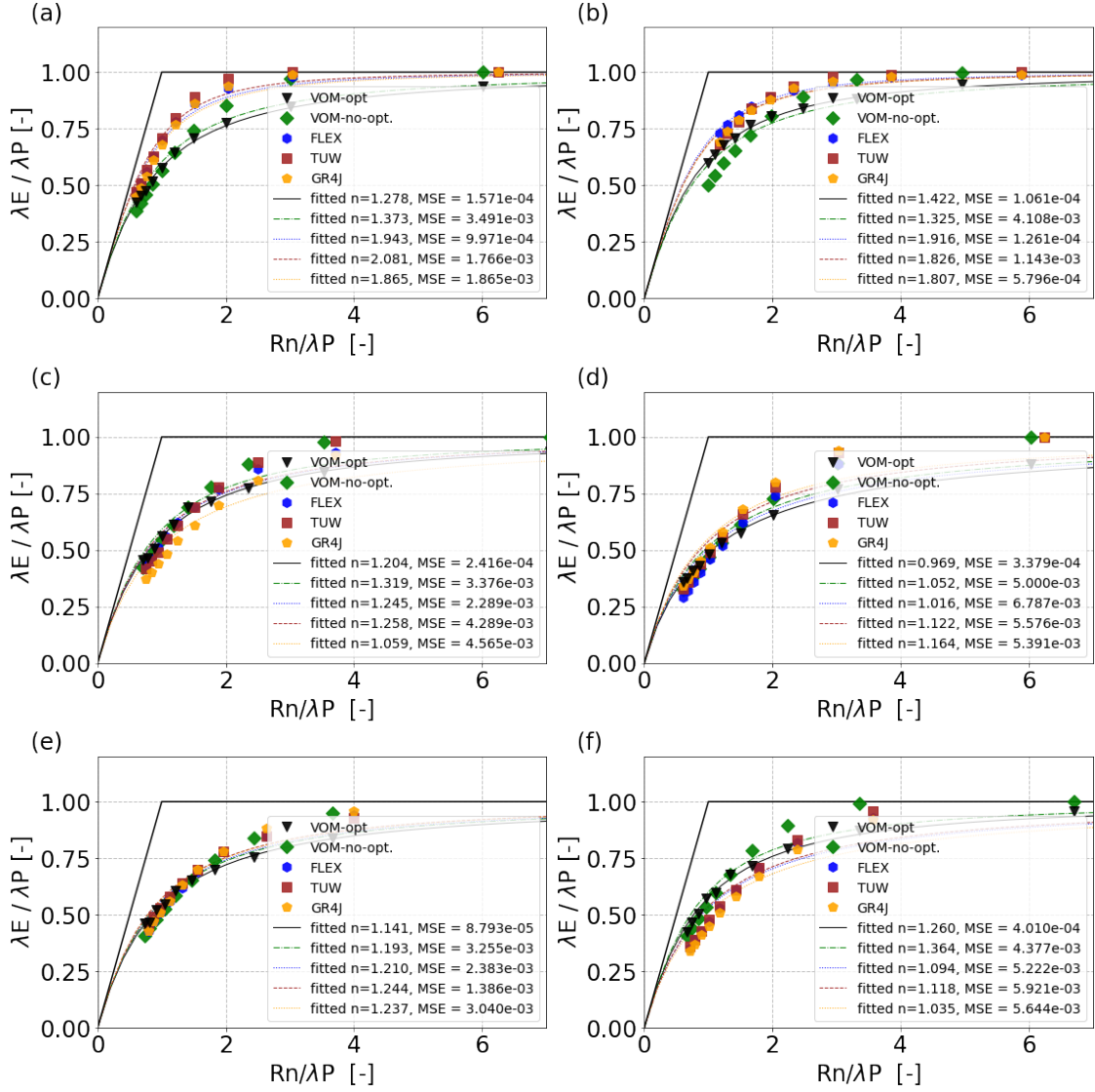


Fig. S3.4. Fitted Budyko-curves for six catchments in Australia with normal and increased precipitation for the optimized VOM (black stars), VOM without optimization (green triangles), FLEX (red diamonds), TUW (gray dots), and GR4J (gold squares) for a) Adelaide River, b) Dry River, c) Fergusson River, d) Magela Creek, e) Seventeen Mile Creek and f) South Alligator River.

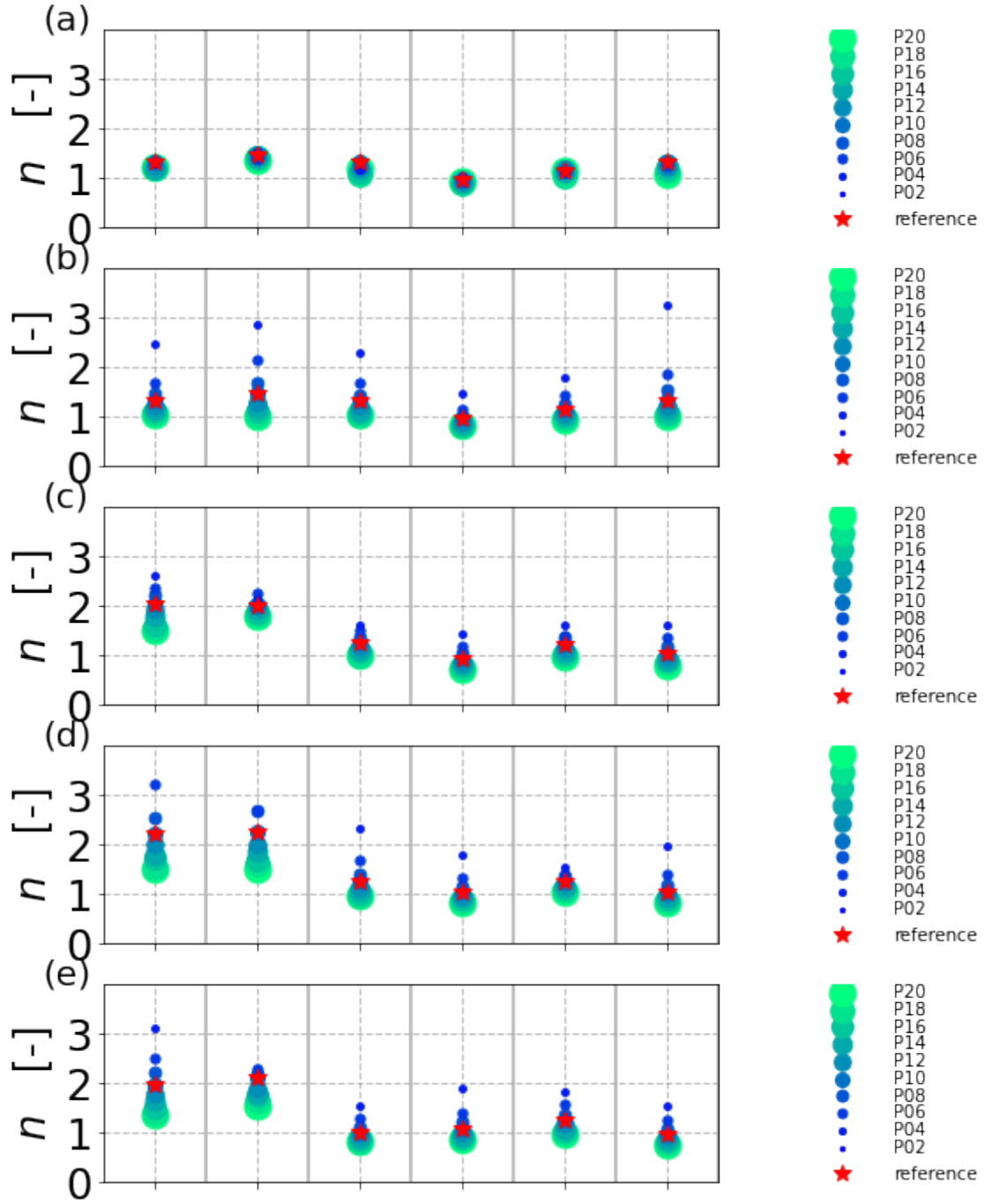


Fig. S3.5. Fitted n -values for six catchments in Australia with normal, reference precipitation (red star) and increased/decreased precipitation (colour scale), for a) the optimized VOM, b) the VOM without optimization, c) FLEX, d) TUW, and e) GR4J.

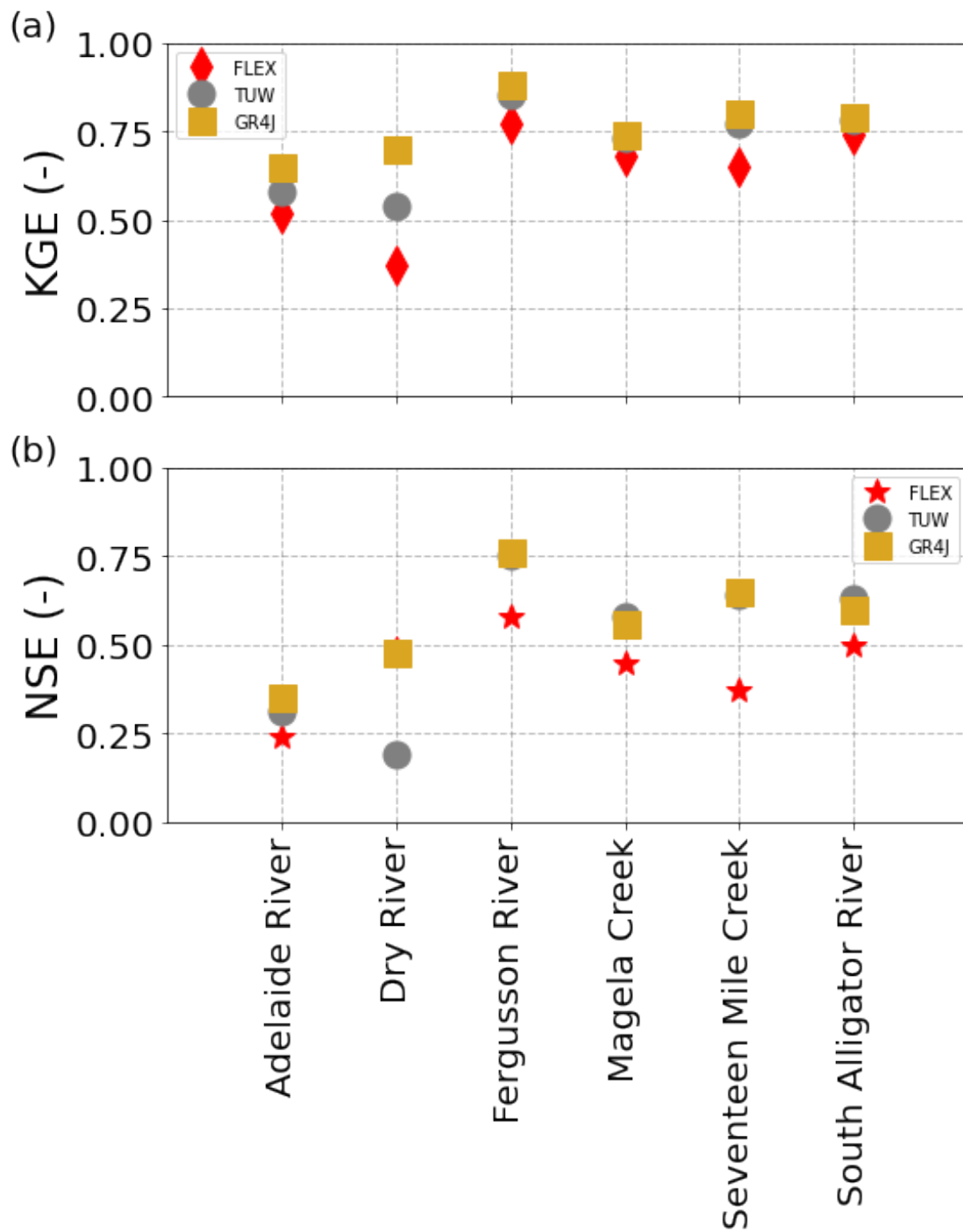


Fig. S3.6. Maximum performances in terms of a) Kling-Gupta efficiency (KGE) and b) Nash-Sutcliffe efficiency (NSE) obtained during calibration for six Australian catchments, for FLEX, TUV and GR4J.

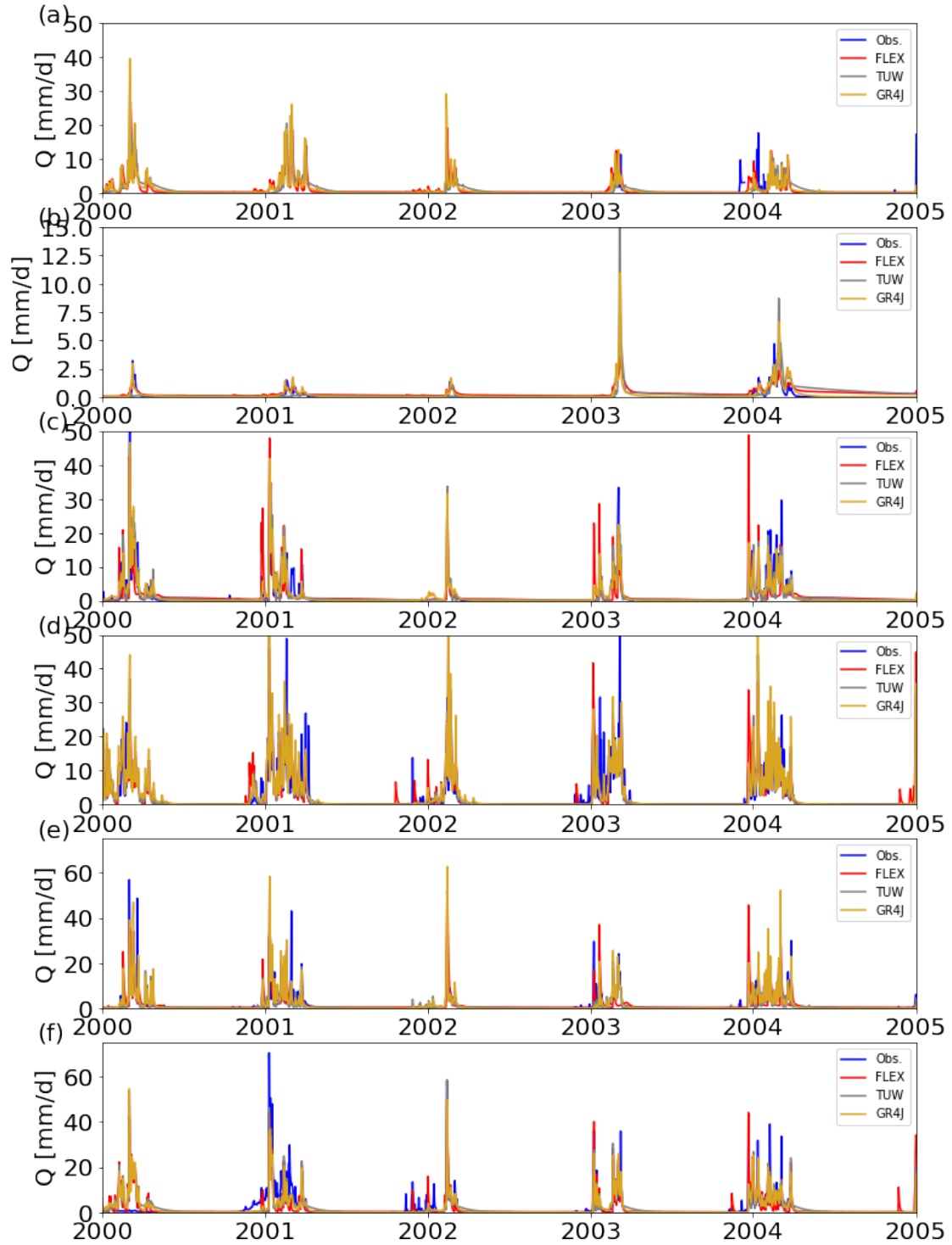


Fig. S3.7. Discharge time series for a) Adelaide River, b) Dry River, c) Fergusson River, d) Magela Creek, e) Seventeen Mile Creek and f) South Alligator River. Observations are shown in blue, FLEX model runs in red, TUW in gray and GR4J in gold.

1.2 CAMELS-data

To investigate the behaviour of the hydrological models for a larger set of catchments with different climates and vegetation, we used the CAMELS-dataset (Addor et al., 2017; Newman et al., 2015). The original data contains 671 catchments across the contiguous United States, but a selection of catchments was made based on the following conditions (similar to Gnann et al. (2019):

- Positive long term mean mean discharge: $\overline{Q} \geq 0$ mm/year.
- Positive long term mean mean precipitation: $\overline{P} \geq 0$ mm/year.
- Runoff ratio smaller than unity: $\frac{\overline{Q}}{\overline{P}} \leq 1$.
- Long term actual evaporation may not exceed potential evaporation: $1 - \frac{\overline{Q}}{\overline{P}} \leq \frac{\overline{E_p}}{\overline{P}}$.
- No lakes: water fraction < 5 %
- No snow-dominated catchments: mean elevation ≤ 2000 m and snow days ≤ 20 %.
- Relatively large catchments: area ≥ 100 km².

This eventually led to a selection of 357 catchments across the contiguous United States. Time series were extracted for each catchment for daily discharge, rainfall, potential evaporation (Priestley and Taylor, 1972) and air temperature to set up the hydrological models.

The models were calibrated by running them with 50,000 random parameterizations. The parameters that achieved the highest Kling-Gupta efficiency (Kling and Gupta, 2008) was considered as the most suitable parameter set. The catchments of the CAMELS data were run for the full length of their time series of approx. 30 years. The catchments in the CAMELS data were evaluated for the full time series after removing one warm-up year.

The models were calibrated for the 357 selected catchments for the unperturbed precipitation. Afterwards, only a single increment in P of 20% was simulated.

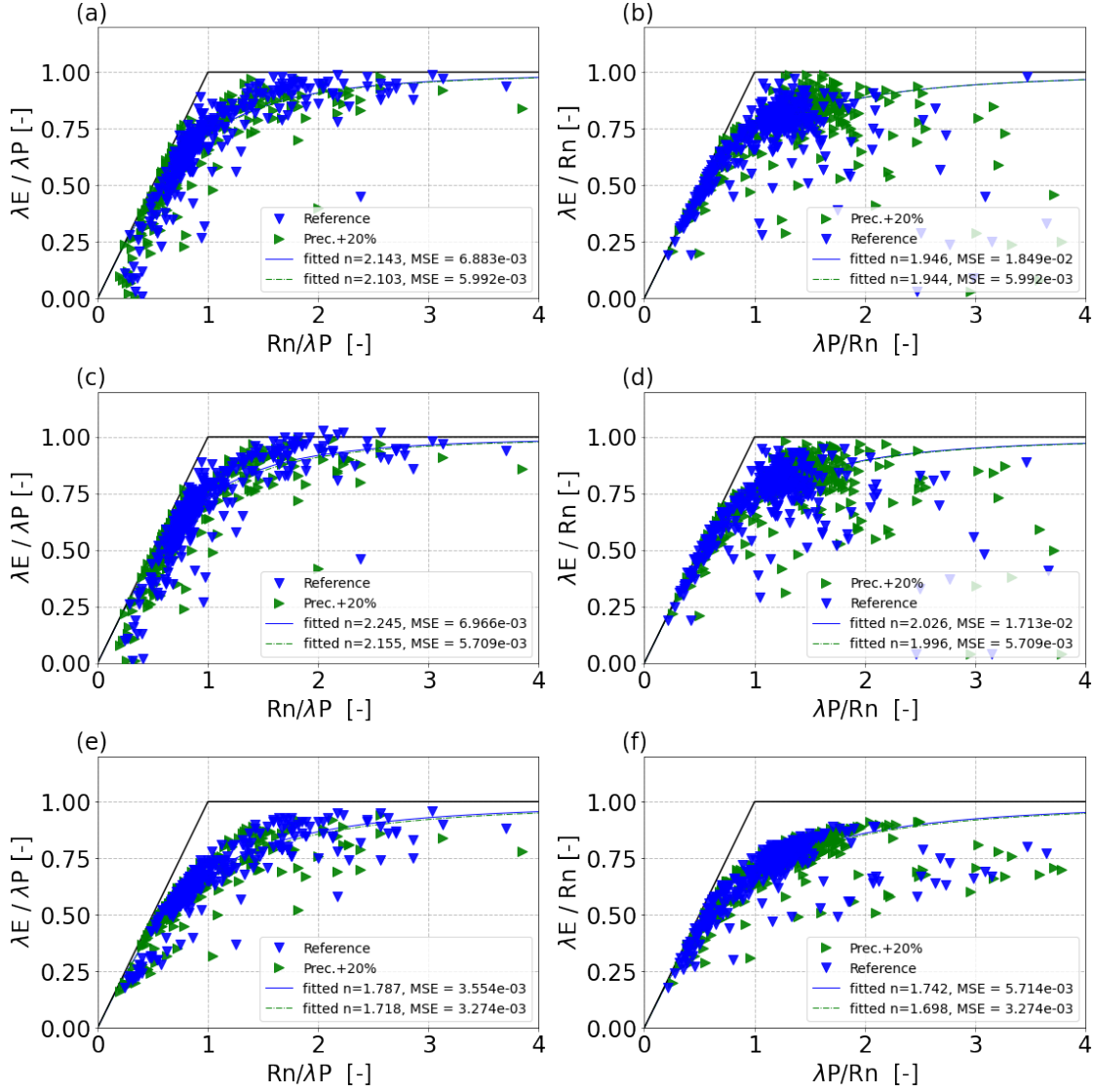


Fig. S3.8. Results of three hydrological models (a-b Flex, c-d TUWmodel and e-f GR4J) in the Budyko-framework for the Camels-data, with in blue the reference runs, and in green the the same runs with increased precipitation, for a), c), e) a Budyko-projection normalized by net radiation, and b), d), e) a Budyko-projection normalized by precipitation.

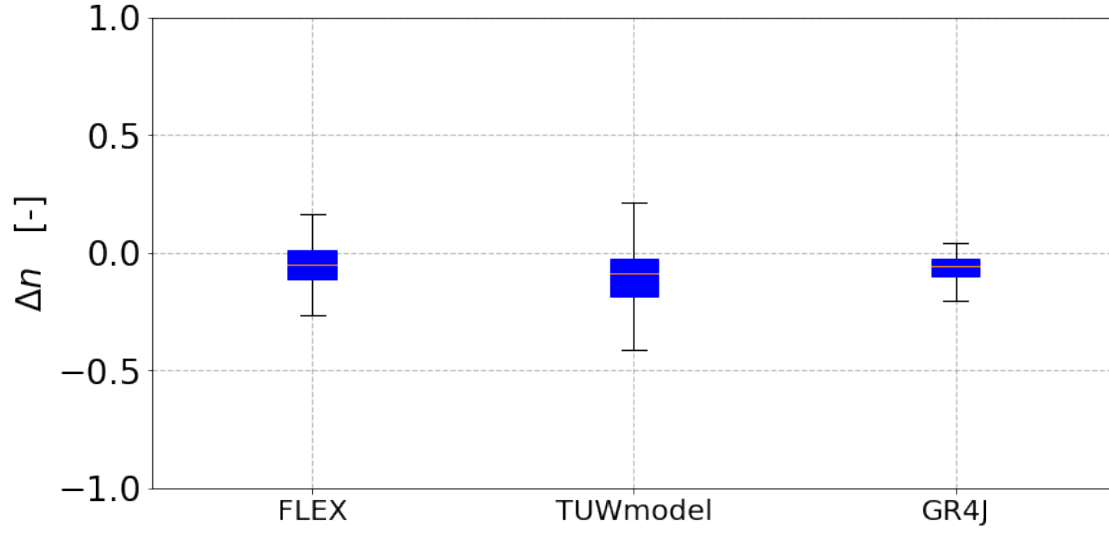


Fig. S3.9. Differences between n -values for normal and increased precipitation, obtained by fitting all hydrological modelling results (for the models FLEX, TUWmodel and GR4J) to an individual Budyko-curve (i.e. per catchment) for a) all Camels-catchments, b) all catchments with an $R_n/\lambda P < 1.0$, and c) all catchments with an $R_n/\lambda P > 1.0$.

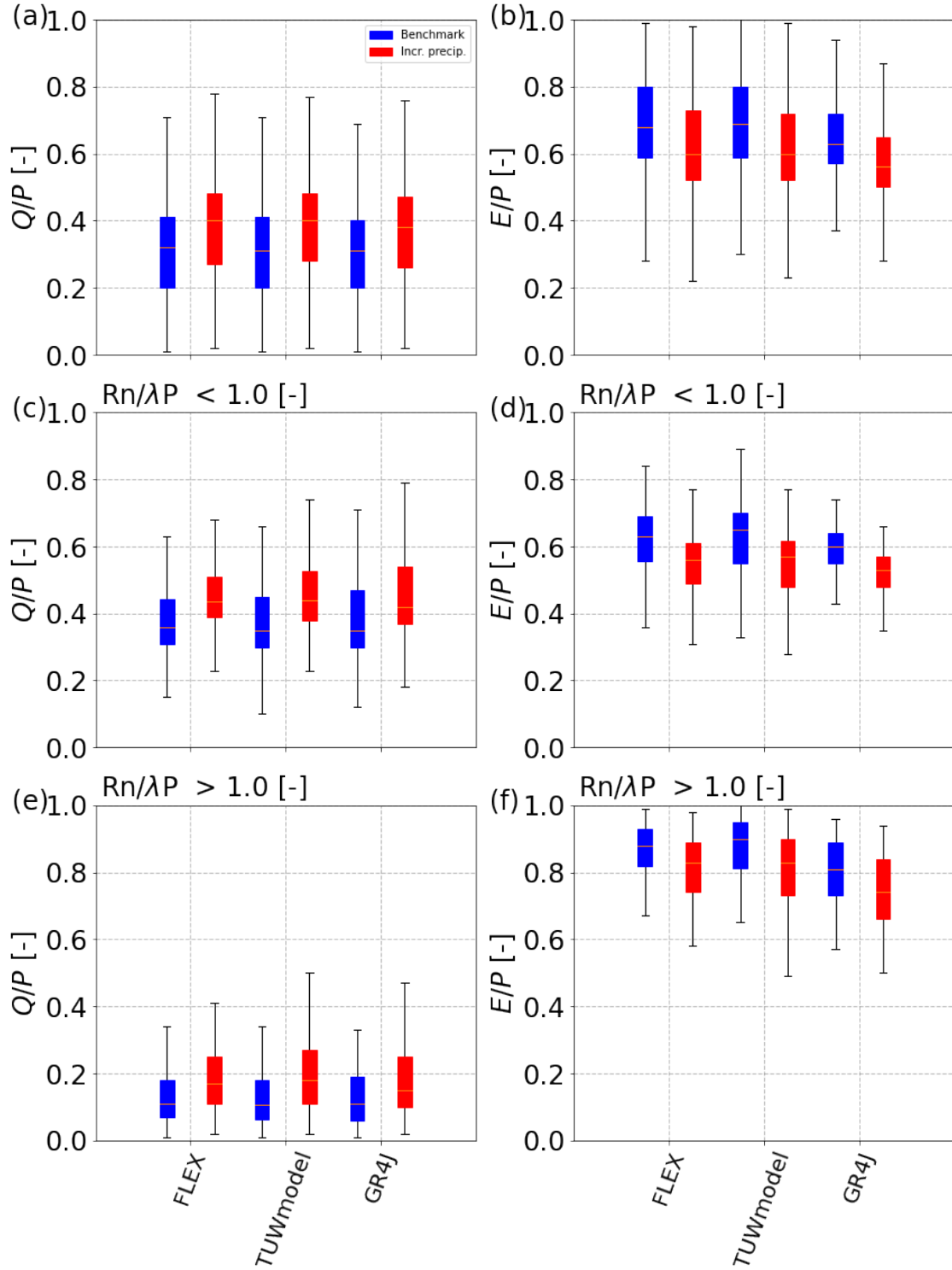


Fig. S3.10. Differences between the runoff ratios and dryness index for normal and increased precipitation, obtained by the models FLEX, TUWmodel and GR4J for a) all Camels-catchments, b) all catchments with an $R_n/\lambda P < 1.0$, and c) all catchments with an $R_n/\lambda P > 1.0$.

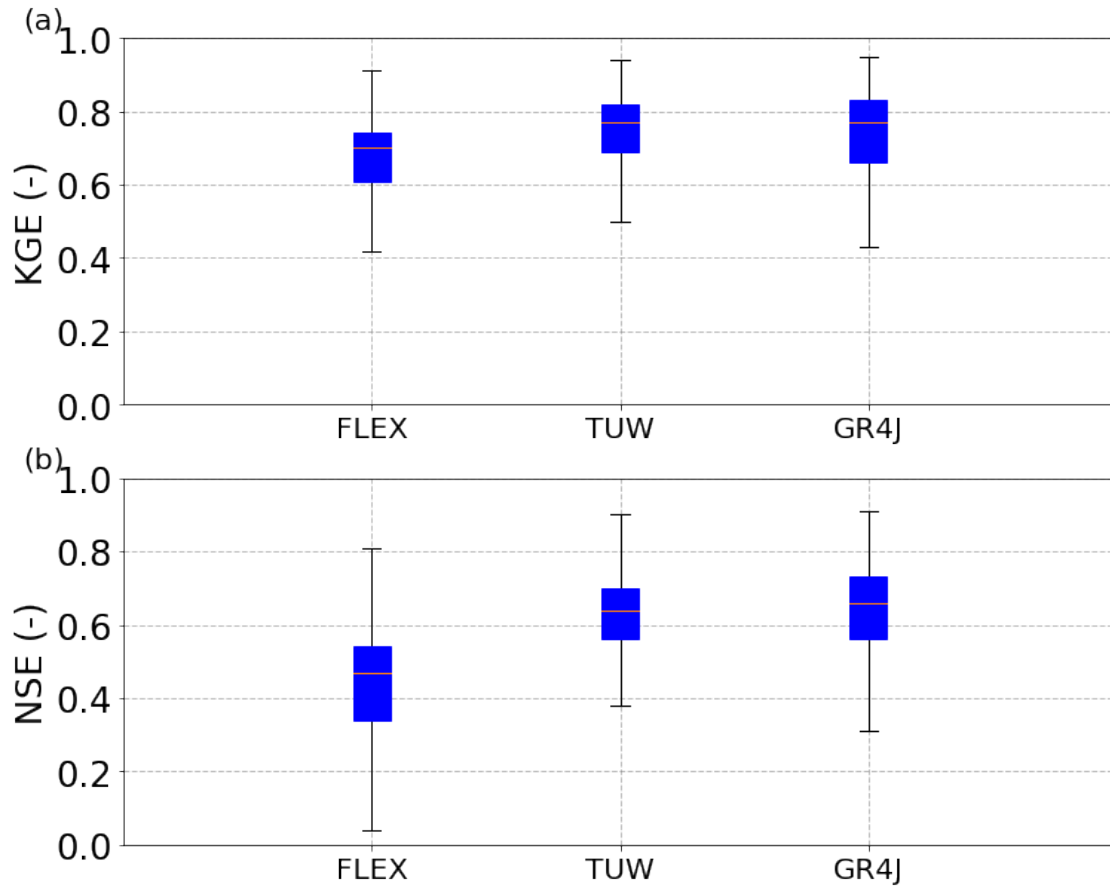


Fig. S3.11. Maximum performances in terms of a) Kling-Gupta efficiency (KGE) obtained during calibration, and b) Nash-Sutcliffe efficiency (NSE) for all CAMELS-catchments, for FLEX, TUV and GR4J.